Int. J. Adv. Appl. Math. and Mech. 3(4) (2016) 49 – 64 (ISSN: 2347-2529)

Journal homepage: www.ijaamm.com

IJAAMM

International Journal of Advances in Applied Mathematics and Mechanics

Influence of magnetic field and thermophoresis on transient forced convective heat and mass transfer flow along a porous wedge with variable thermal conductivity and variable Prandtl number

Research Article

ATM. M. Rahman[a], **M. S. Alam**[b, *], **M. J. Uddin**[c]

[a] Department of Computer Science and Engineering,Dhaka International University, Dhaka-1205, Bangladesh

[b] Department of Mathematics, Jagannath University, Dhaka-1100, Bangladesh

[c] Department of Mathematics and Statistics, College of Science, Sultan Qaboos University, P. O. Box 36, P. C. 123, Al-Khod, Muscat, Sultanate of Oman

Received 07 April 2016; accepted (in revised version) 12 May 2016

Abstract: In this paper, the influence of magnetic field and thermophoresis on unsteady two-dimensional forced convective heat and mass transfer flow of a viscous, incompressible and electrically conducting fluid along a porous wedge in the presence of the temperature-dependent thermal conductivity and variable Prandtl number have been studied numerically. The governing nonlinear partial differential equations have been transformed into nonlinear ordinary one by introducing a similarity transformation. The transformed ordinary differential equations are solved for similar solutions by applying Nachtsheim- Swigert shooting iteration technique along with the Runge-Kutta integration scheme. Comparison with beforehand published work is performed and excellent agreement is found. Results for the dimensionless velocity, temperature, concentration, thermophoretic velocity and thermophoretic particle deposition velocity are presented for various parametric conditions. The numerical results show that the thermophoretic particle deposition velocity significantly influenced by the magnetic field parameter. Moreover, it is found that the rate of heat transfer significantly influenced by the variation of the thermal conductivity and Prandtl number. Thus, in any physical model where thermal conductivity of the fluid is temperature dependent, the Prandtl number within the boundary layer must be treated as variable rather than constant.

MSC: 76D05 • 65L60

Keywords: Thermophoresis • Unsteady flow • Variable thermal conductivity • Variable Prandtl number

1. Introduction

Thermophoresis is a radiometric force by temperature gradient that enhances small particles moving toward a cold surface and away from a hot one. The effect of thermophoresis on small particle size is especially effective in a range of $0.1\mu m - 1.0\mu m$. This phenomenon has many engineering applications, such as removing small particles from gas streams, particle deposition on to a wafer surface in the modern semiconductor industry, electronic component cooling using a fan, filtration process in gas- cleaning problems for nuclear reactor safety, clean room and human healthy topics, etc. Thermophoresis plays a vital role in the mass transfer mechanism for the chemical vapor deposition process used during the fabrication of optical fibers. Due to the practical importance to thermophoresis phenomenon, many researchers (Goldsmith and May [1], Kanki et al. [2], Shen [3], Vajravelu and Nayfeh [4], Konstandopoulos [5], Chang et al. [6], Anjjali Devi and Kandasamy [7], Chamkha and Pop [8], Chamkha et al. [9], Postelnicu [10], Alam et al. [11], Rahman and Postelnicu [12] have studied and reported results on this topic considering various

* Corresponding author.

E-mail addresses: atmmrahman2005@gmail.com (ATM. M. Rahman), dralamjnu@gmail.com (M. S. Alam), jashim.fluidm@gmail.com (M. J. Uddin)

flow conditions in different geometries. Konstandopoulos and Rosner [13] and Tsai [14] reported correlations for predicting the deposition rate in the presence of thermophoresis. Recently, Alam and Rahman [15] analyzed the effect of variable heat and mass fluxes on hydromagnetic free convection and mass transfer flow along an inclined permeable stretching surface with thermophoresis.

The study of magnetohydrodynamic (MHD) flow of an electrically conducting fluid is of considerable interest in modern metallurgical and metal-working processes. The study of MHD flow and heat transfer are deemed as of great interest due to the effect on the magnetic field on the boundary-layer flow control and on the performance of many systems using electrically conducting fluids. Some of the engineering applications are in MHD generators, plasma studies, nuclear reactor, geothermal energy extractions, and purifications of metal from non-metal enclosures, polymer technology and metallurgy. Various industrial heat transfer processes involved the hydromagnetic flows and thermophoresis such as in MHD energy systems, magnetohydrodynamic heat and mass transfer systems. Some examples of investigations dealing with hydromagnetic flows over a surface can be found throughout the work of Watanabe and Pop [16], Chandran et al. [17], Yih [18]-[19], Rahman et al. [20] and Muhaimin et al. [21]. In all these studies, the thermo-physical properties of the fluid, especially the thermal conductivities were assumed to be constant. However, it is well known that the thermal conductivity of fluid may change with temperature Chiam [22]-[23]. Prasad and Vajravelu [24] performed the effect of variable thermal conductivity in a non-isothermal sheet stretching through power law fluids. Abel et al. [25] investigated the combined effects of thermal buoyancy and variable thermal conductivity on a magnetohydrodynamic flow and the associated heat transfer through a power-law fluid past a vertical stretching sheet in the presence of a non-uniform heat source. Both studies revealed that the variable thermal conductivity increased the wall shear stress. Recently, Vajravelu et al. [26] discussed the unsteady convective boundary-layer flow of a viscous fluid at a vertical surface with variable fluid properties.

The thickness of the thermal boundary layer relative to the velocity boundary layer depends upon the Prandtl number which by its definition varies inversely with the thermal conductivity of the fluid. As the thermal conductivity varies with temperature so does the Prandtl number. Despite this fact, all the afore-mentioned studies treated the Prandtl number as a constant. The use of a constant Prandtl number within the boundary layer when the thermal conductivities of fluid are temperature dependent, introduces errors in the computed results. Rahman et al. [27] focused on heat transfer in micropolar fluid along an inclined permeable plate considering variable thermal conductivity and variable Prandtl number. Recently, Rahman and Eltayeb [28] initiated the effect of variable thermal conductivity and variable Prandtl number on convective slip flow of rarefied fluids over a wedge with thermal jump. Both studies confirmed that in modeling, the thermal boundary-layer flow when the thermal conductivities of fluid are temperature dependent, the Prandtl number must be treated as a variable to obtain realistic results.

Therefore, the aim of the present study is to investigate the effects of magnetic field and thermophoresis on an unsteady two-dimensional forced convective heat and mass transfer flow along a permeable wedge taking into account the variable thermal conductivity. Thus, one of the main focuses behind this study is also to investigate how the Prandtl number varies within the boundary layer when the thermal conductivity depends linearly on temperature. By introducing of similarity transformations proposed by Sattar [29], the governing non-linear partial differential equations have been reduced to locally similar ordinary differential equations, which are solved numerically using Nachtsheim-Swigert shooting iteration procedure. Graphs and table are presented to show the important features of the solution.

2. Mathematical model

We consider an unsteady two-dimensional laminar forced convective heat and mass transfer flow of a viscous incompressible electrically conducing fluid along a porous wedge. The angle of the wedge is given by $\Omega = \beta\pi$ as shown in Fig. 1. The surface of the wedge is maintained at a constant temperature T_w and constant concentration C_w which are higher than the ambient temperature T_∞ and ambient concentration C_∞, respectively. The x-axis is taken along the direction of the wedge and y-axis normal to it. In addition, a uniform transverse magnetic field of strength B_0 is applied parallel to the y-axis. Viscous dissipation and Joule heating terms have been considered in the energy equation. Besides, fluid suction or injection is imposed on the wedge surface. The thermal conductivity of the fluid is assumed to be a function of temperature. Then under the boundary layer approximation the governing equations for this problem are as follows (see also Rahman et al. [30]-[31]:

$$\frac{\partial u}{\partial x} + \frac{\partial v}{\partial y} = 0 \tag{1}$$

$$\frac{\partial u}{\partial t} + \frac{\partial (u^2)}{\partial x} + \frac{\partial (uv)}{\partial y} = -\frac{1}{\rho}\frac{\partial p}{\partial x} + \nu\frac{\partial^2 u}{\partial y^2} - \frac{\sigma B_0^2}{\rho}(u-U) \tag{2}$$

$$\frac{\partial T}{\partial t} + \frac{\partial (uT)}{\partial x} + \frac{\partial (vT)}{\partial y} = \frac{1}{\rho c_p}\frac{\partial}{\partial y}(k_f\frac{\partial T}{\partial y}) + \frac{\mu}{\rho c_p}(\frac{\partial u}{\partial y})^2 + \frac{\sigma B_0^2}{\rho c_p}(u-U)^2 \tag{3}$$

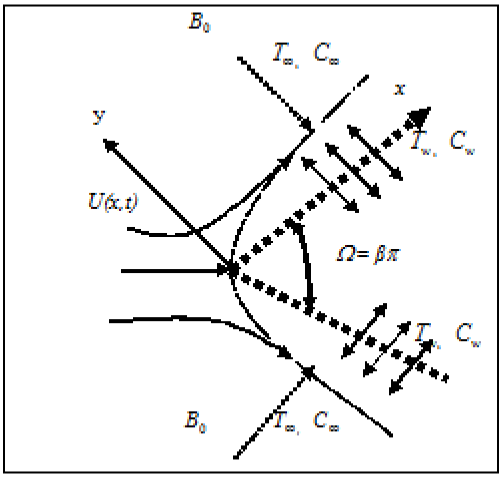

Fig. 1. Flow configuration and co-ordinate system.

$$\frac{\partial C}{\partial t}+\frac{\partial (uC)}{\partial x}+\frac{\partial (vC)}{\partial y}=D\frac{\partial^2 C}{\partial y^2}-\frac{\partial}{\partial y}(V_T C) \tag{4}$$

where the variables and related quantities have their usual meanings. In boundary-layer flow, the temperature gradient in the y -direction is much larger than that in the x -direction and hence only the thermophoretic velocity in y -direction is considered. As a consequence, in Eq. (4), the thermophoretic velocity V_T, was recommended by Talbot et al. [32]

$$V_T=-\frac{\kappa \nu}{T}\frac{\partial T}{\partial y} \tag{5}$$

where $\kappa\nu$ represents the thermophoretic diffusivity and κ is the thermophoretic coefficient which ranges in value from 0.2 to 1.2 as indicated by Batchelor and Shen [33] and is defined by

$$\kappa=\frac{2C_s(k_f/\lambda_p+C_t Kn)C_c}{(1+3C_m Kn)(1+2k_f/\lambda_p+2C_t Kn)} \tag{6}$$

where k_f and λ_p are the thermal conductivities of the fluid and diffused particles, respectively. $C_m = 1.146$, $C_s = 1.147$, $C_t = 2.20$ are constants obtained from the experimental data. $C_c = [1+Kn(C_1+C_2 e^{-C3/Kn})]$ is the Stokes-Cunningham correction factor, Kn is the Knudsen number, $C_1 = 1.2$, $C_2 = 0.41$, and $C_3 = 0.88$.

3. Boundary conditions

The boundary conditions for the above stated model are as follows:

$$u=0 \quad v=\pm v_w(x,t), \quad T=T_w \quad C=C_w \quad at \quad y=0 \tag{7}$$

$$u=U(x,t) \qquad T\to T_\infty, \qquad C\to C_\infty \qquad as \qquad y\to\infty \tag{8}$$

where $v_w(x,t)$ represents the suction/ injection velocity at the porous surface where its sign indicates suction (<0) or injection (>0) and $U(x,t)$ is the potential velocity generated by the wedge. The potential flow velocity for the wedge flow (see Sattar [29]) is taken as:

$$U(x,t)=\frac{\nu x^m}{\delta^{m+1}} \tag{9}$$

where m is an arbitrary constant and is related to the wedge angle and δ is the time-dependent length scale which is taken to be (more detailed in Sattar [34]) as:

$$\delta=\delta(t) \tag{10}$$

4. Dimensional analysis

Dimensional analysis is one of the most important mathematical tools in the study of fluid mechanics. To describe several transport mechanisms that appear in fluid dynamics problems, it is meaningful to make the conservation equations into non-dimensional form. The advantages of non-dimensionalization are as follows: (i) Non-dimensionalization gives you freedom to analysis for any system irrespective of their material properties. (ii) one can easily understand the controlling flow parameters of the system, (iii) make a generalization of the size and shape of the geometry, and (iv) before doing experiment one can get insight of the physical problem. These aims can be achieved through the appropriate choice of scales. Therefore,in order to obtain the dimensionless form of the governing Eqs. (1)-(4) together with the boundary conditions (7)-(8), we introduce the following non-dimensional variables:

$$\eta = y\sqrt{\frac{m+1}{2}}\sqrt{\frac{x^{m-1}}{\delta^{m+1}}},\quad \psi = \sqrt{\frac{2}{m+1}\frac{\nu x^{(m+1)/2}}{\delta^{(m+1)/2}}}f(\eta),\quad \theta(\eta) = \frac{T-T_\infty}{T_w-T_\infty},\quad \phi(\eta) = \frac{C-C_\infty}{C_w-C_\infty} \tag{11}$$

where η is the similarity variable, ψ is the stream function that satisfies the continuity Eq. (1) and is defined by $u = \frac{\partial\psi}{\partial y}$ and $v = -\frac{\partial\psi}{\partial x}$. Since $u = \frac{\partial\psi}{\partial y}$ and $v = -\frac{\partial\psi}{\partial x}$, we have from Eq. (11)

$$u = U(x,t)f' \tag{12}$$

and

$$v = -\sqrt{\frac{2}{m+1}}\frac{(m+1)}{2}\frac{\nu x^{(m-1)/2}}{\delta^{(m+1)/2}}\left(f + \frac{m-1}{m+1}\eta f'\right) \tag{13}$$

where f is non dimensional stream function and prime denotes differentiation with respect to η. The model Chiam [22]-[23] for a variable thermal conductivity is considered as:

$$k_f = k_\infty(1+\gamma\frac{T-T_\infty}{T_w-T_\infty}) \tag{14}$$

where k_∞ is the thermal conductivity of the ambient fluid and γ is the thermal conductivity variation parameter. Now employing the Eqs. (11)-(14) into Eqs. (2)-(4), we obtain the following nonlinear ordinary differential equations:

$$f''' + ff'' + \beta(1-f'^2) - (\frac{\delta^m}{\nu x^{m-1}}\frac{d\delta}{dt})(2-2f'-\eta f'') - \frac{2}{m+1}Ha^2(f'-1) = 0 \tag{15}$$

$$\theta'' + \frac{\gamma}{1+\gamma\theta}\theta'^2 + \frac{Pr_\infty}{1+\gamma\theta}f\theta' + (\frac{\delta^m}{\nu x^{m-1}}\frac{d\delta}{dt})\frac{Pr_\infty}{1+\gamma\theta}\eta\theta' + \frac{Pr_\infty}{1+\gamma\theta}Ec(f'')^2 + \frac{Pr_\infty}{1+\gamma\theta}EcHa^2(f'-1)^2 = 0 \tag{16}$$

$$\phi'' + Scf\phi' + (\frac{\delta^m}{\nu x^{m-1}}\frac{d\delta}{dt})Sc\eta\phi' + \frac{\kappa Sc}{N_t+\theta}[(N_c+\phi)\theta'' + \theta'\phi' - (\frac{N_c+\phi'}{N_t+\theta})\theta'^2] = 0 \tag{17}$$

with the transformed boundary conditions:

$$f = f_w,\quad f' = 0,\quad \theta = 1\quad \phi = 1\quad at\quad \eta = 0 \tag{18}$$

$$f' = 1,\quad \theta = 0\quad \phi = 0\quad as\quad \eta\to\infty \tag{19}$$

The dimensionless parameters appear in the above-equations are defined as: $\beta = \frac{2m}{m+1}$ is the wedge angle parameter that corresponds to $\Omega = \beta\pi$ for a total angle Ω of the wedge, $Pr_\infty = \frac{\mu c_p}{k_\infty}$ (where $\nu = \frac{\mu}{\rho}$) is the ambient Prandtl number, $Sc = \frac{\nu}{D}$ is Schmidt number, $N_t = \frac{T_\infty}{T_w-T_\infty}$ is the thermophoresis parameter, $N_c = \frac{C_\infty}{C_w-C_\infty}$ is the concentration ratio, $Ha = B_0\sqrt{\frac{\sigma x}{\rho U}}$ is the local Hartman number, $Ec = \frac{U}{c_p(T_w-T_\infty)}$ is the Eckert number and $f_w = -\frac{v_w(x,t)}{\left(\sqrt{\frac{(m+1)}{2}\frac{\nu x^{\frac{m-1}{2}}}{\delta^{\frac{m+1}{2}}}}\right)}$ is the wall mass transfer coefficient which is positive ($f_w > 0$) for suction and negative ($f_w < 0$) for injection.

Now in order to make Eqs. (15)-(17) locally similar, let

$$\frac{\delta^m}{\nu x^{m-1}}\frac{d\delta}{dt}=\lambda \tag{20}$$

where λ is taken to be a constant and thus can be treated as a dimensionless measure of the unsteadiness. Hence Eqs. (15)-(17) become

$$f'''+ff''+\beta(1-f'^2)-\lambda(2-2f'-\eta f'')-\frac{2}{m+1}Ha^2(f'-1)=0 \tag{21}$$

$$\theta''+\frac{\gamma}{1+\gamma\theta}\theta''+\frac{Pr_\infty}{1+\gamma\theta}f\theta'+\lambda\frac{Pr_\infty}{1+\gamma\theta}\eta\theta'+\frac{Pr_\infty}{1+\gamma\theta}Ec(f'')^2+\frac{Pr_\infty}{1+\gamma\theta}EcHa^2(f'-1)^2=0 \tag{22}$$

$$\phi''+Scf\phi'+\lambda Sc\eta\phi'+\frac{\kappa Sc}{N_t+\theta}[(N_c+\phi)\theta''+\theta'\phi'-(\frac{N_c+\phi'}{N_t+\theta})\theta'^2]=0 \tag{23}$$

Further, we suppose that $\lambda=\frac{c}{x^{m-1}}$, where c is a constant so that

$$c=\frac{\delta^m}{\nu}\frac{d\delta}{dt} \tag{24}$$

Thus integrating Eq. (24) we obtain that

$$\delta=[c(m+1)\nu t]^{\frac{1}{m+1}} \tag{25}$$

Now taking $c=2$ and $m=1$ in Eq. (25) we obtain

$$\delta=2\sqrt{\nu t} \tag{26}$$

The length scales $2\sqrt{\nu t}$ for the ordinate similar to one seen in Eq. (26) was initially used by Stokes [35] for an unsteady parallel flow, but $\delta(t)$ form of the length scale was initially developed by Sattar and Hossain [34] in case of a solution of an unsteady one- dimensional boundary-layer problem. The characteristics length scale $\delta(t)$ defined particularly in Eq. (26) physically related to the boundary-layer thickness which can be viewed in Schlichting [36], Alam and Huda [37], Alam [38], Alam et al. [39].

5. Variable Prandtl number

From the definition of Prandtl number, we see that it is a function of viscosity, thermal conductivity and specific heat. However, since the thermal conductivity varies across the boundary layer, the Prandtl number also varies. The assumption of constant Prandtl number inside the boundary layer when thermal conductivities are temperature-dependent leads to unrealistic results (more detailed in Rahman et al. [28] and Rahman and Eltayeb [29]). Therefore, in the present work, the Prandtl number related to the variable thermal conductivity is defined as:

$$Pr_v=\frac{\mu c_p}{k_f}=\frac{\mu c_p}{k_\infty(1+\gamma\theta)}=\frac{Pr_\infty}{(1+\gamma\theta)} \tag{27}$$

At the surface ($\eta=0$) of the wedge, this can be written as $Pr_w=\frac{Pr_\infty}{1+\gamma}$.

From Eq. (27), it can be seen that for $\gamma\to 0$, the variable Prandtl number Pr_v is equal to the ambient Prandtl number Pr_∞. It is mention that for $\eta\to\infty$, i.e. outside the boundary layer, $\theta(\eta)$ becomes zero; therefore, $Pr_v=Pr_\infty$ regardless of the values of γ.

Table 1 shows that the variation of the Prandtl number at the surface of the wedge for several values of γ for a fixed value of the ambient Prandtl number $Pr_\infty=0.71$. From this table, it is observed that Prandtl number at the surface of the wedge Pr_w decreases as γ increases. The value of thermal conductivity variation parameter γ is increased from 0.0 to 7.0 when the Prandtl number decreased by 87.46%.

In light of the above discussion and using Eq. (27), the non-dimensional temperature Eq. (22) can be expressed as:

$$\theta''+\frac{\gamma}{1+\gamma\theta}\theta''+Pr_vf\theta'+\lambda Pr_v\eta\theta'+Pr_vEc(f'')^2+Pr_vEcHa^2(f'-1)^2=0 \tag{28}$$

Eq. (28) is the corrected non- dimensional form as the energy equation in which Prandtl number is treated as a variable (see also Rahman et al. [28] and Rahman and Eltayeb [29]).

6. Parameters of engineering interest

The parameters of engineering interest for the present problem are the local skin friction coefficient; wall heat transfer rate, the thermophoretic velocity and wall thermophoretic particle deposition velocity. These can be obtained from the following expressions.
Local skin-friction coefficient:

$$\frac{1}{2}C_f\sqrt{2-\beta}=Re^{-\frac{1}{2}}f''(0) \tag{29}$$

Local Nusselt number:

$$Nu\sqrt{2-\beta}=-Re^{\frac{1}{2}}\theta'(0) \tag{30}$$

The non-dimensional thermophoretic velocity are evaluated as

$$V_{TW}=-\sqrt{\frac{1}{2-\beta}}Re^{\frac{1}{2}}\frac{\kappa}{1+N_t}\theta'(0) \tag{31}$$

The thermophoretic particle deposition velocity at the surface of the wedge is evaluated by

$$V_d=-\sqrt{\frac{1}{2-\beta}}\frac{1}{Sc}Re^{\frac{1}{2}}\frac{\nu}{x}\phi'(0) \tag{32}$$

Therefore non-dimensional thermophoretic particle deposition velocity is obtained by

$$V_d^*=\frac{V_d x}{\nu}=-\sqrt{\frac{1}{2-\beta}}\frac{1}{Sc}Re^{\frac{1}{2}}\phi'(0) \tag{33}$$

where $Re=\dfrac{Ux}{\nu}$ is the local Reynold's number.

7. Numerical experiment

The locally similar and nonlinear ordinary differential Eqs. (21), (23) and (28) with the boundary conditions (18)-(19) are solved using shooting iteration technique (See Nachtsheim and Swigert [40] and Alam et al.[41]. Thus adopting this numerical technique, a computer program was set up for the solutions of the governing non-linear ordinary differential equations of our problem with Runge-Kutta method of integration. A step size of $\Delta\eta=0.01$ was selected to be satisfactory for a convergence criterion of 10^6 in all cases.

7.1. Code verification

To check the validity of the present code, we have calculated the values of $f(0)$, $f'(0)$ and $f''(0)$ for the Falkner-Skan boundary-layer equation for the case $\gamma=0$ (for constant fluid thermal conductivity), $\beta=0$, $Ha=0$, $f_w=0$ (impermeable wedge) and $\lambda=0$ (for steady flow) for different values of η . Thus from Table 2, we observe that the data produced by the present code and those of White [42] are in excellent agreement, which gives us confidence to use the present numerical code.

Table 1. Values of Pr_w versus γ for $Pr_\infty=0.71$ at $\eta=0$.

γ	0.00	0.50	1.0	3.0	5.0	7.0
Pr_w	0.71	0.437	0.355	0.177	0.118	0.089

Table 2. Comparison of the present numerical results of Falkner-Skan boundary layer equation for the case of $\beta = \gamma = f_w = Ha = 0$ and $\lambda = 0$.

η	$f(\eta)$		$f'(\eta)$		$f''(\eta)$	
	present work	White[42]	present work	White[42]	present work	White[42]
0.0	0.0000000	0.00000	0.00000000	0.00000	0.46964218	0.46960
0.5	0.05865082	0.05864	0.23424831	0.23423	0.46507107	0.46503
1.0	0.23301626	0.23299	0.46067192	0.46063	0.43441274	0.43438
1.5	0.51508336	0.51503	0.66152592	0.66147	0.36182459	0.36180
2.0	0.88687819	0.88680	0.81675164	0.81669	0.25567446	0.25567
3.0	1.79570660	1.79557	0.96910685	0.96905	0.06770503	0.06771
4.0	2.78407530	2.78388	0.99781828	0.99777	0.00687281	0.00687
5.0	3.78347123	3.78323	0.99998350	0.99994	0.00025771	0.00026

Table 3. Variations of thermophoretic particle deposition velocity at the wall for several values of Sc.

f_w	Sc	$(V_d^* Re^{-\frac{1}{2}})$
0.5	0.22	1.464883
0.5	0.30	1.251766
0.5	0.60	0.890707
0.5	0.94	0.718497
−0.5	0.22	1.116588
−0.5	0.30	0.906355
−0.5	0.60	0.556096
−0.5	0.94	0.391592

Table 4. Numerical values of $-\theta'(0)$ for various values of γ and f_w.

f_w	γ	$-\theta'(0)(VPr)$	$-\theta'(0)(CPr)$	Error= $\left\lvert\frac{VPr-CPr}{VPr}\right\rvert \times 100$
0.5	0.0	0.902102	0.902102	0.00%
0.5	1.0	0.675392	0.551469	18.35%
0.5	2.0	0.599989	0.423934	29.34%
0.5	3.0	0.562266	0.355324	36.08%
0.5	5.0	0.524614	0.280500	46.53%
0.5	7.0	0.505784	0.238762	52.79%
0.5	9.0	0.494490	0.211389	57.25%
−0.5	0.0	0.426180	0.426180	0.00%
−0.5	1.0	0.318993	0.313947	1.58%
−0.5	2.0	0.283352	0.264757	6.56%
−0.5	3.0	0.265515	0.235251	11.40%
−0.5	5.0	0.247676	0.199283	19.54%
−0.5	7.0	0.238789	0.177172	25.80%
−0.5	9.0	0.223472	0.161631	30.77%

8. Results and discussion

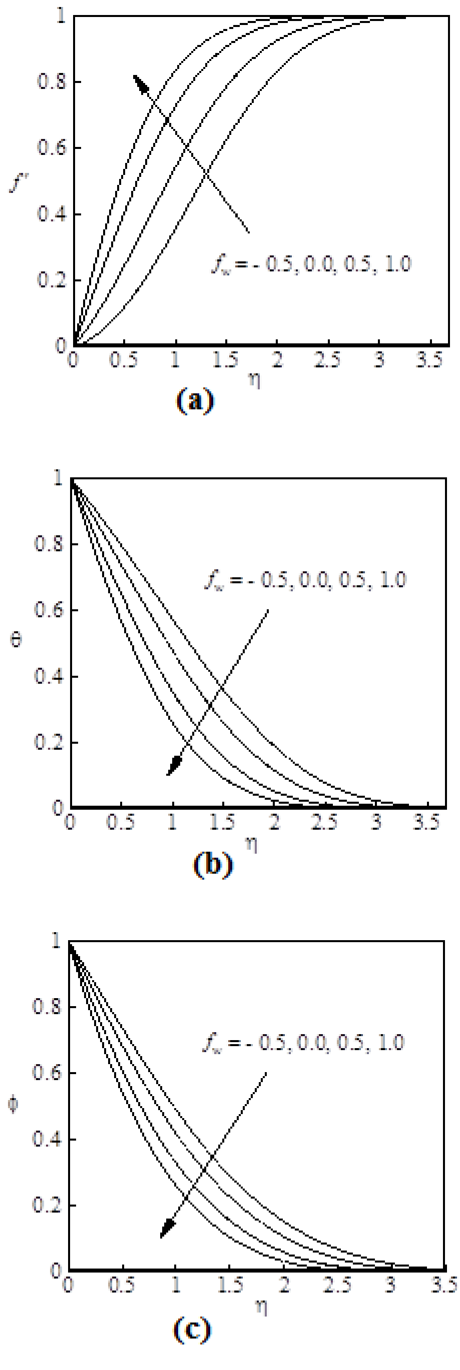

Fig. 2. Variation of dimensionless (a) velocity, (b) temperature and (c)concentration profiles for several values of f_w.

Numerical values of velocity, temperature, concentration and thermophoretic velocity are presented graphically for different values of the mass transfer coefficient $f_w = -0.5$ to 1.0, Hartman number $Ha = 0$ (non-magnetic) to 4, thermal conductivity variation parameter $\gamma = 0$ (constant thermal conductivity) to 7, unsteadiness parameter $\lambda = 0.5-2.5$, Schmidt number $Sc = 0.22-0.94$, concentration ratio $N_c = 2-5$, thermophoresis parameter $N_t = 2-50$, wedge angle parameter $\beta = 0-4$, thermophoretic coefficient $\kappa = 0.2-1.2$. When thermal conductivity does not depend on the temperature, the values of the ambient Prandtl number, $Pr_\infty = 0.71, 1, 2.97, 4.24,$ and 7.02 correspond to air, electrolyte solution such as salt water, methyl chloride, sulfur dioxide and water at 20^0C. When thermal conductivity depends on the temperature, these values at the surface of the wedge ($\eta = 0$) and for $\gamma = 0.5$ correspond to 0.47, 0.66, 1.98, 2.83, and 4.68, respectively. The value of Eckert number is taken $Ec = 0.02$ whereas the values of Schmidt number Sc are taken for hydrogen ($Sc = 0.22$), helium ($Sc = 0.30$), water-vapor ($Sc = 0.60$), Carbon-Dioxide ($Sc = 0.94$).

Fig. 2 (a)-(c) depict the influence of the wall mass transfer coefficient f_w on the velocity, temperature and con-

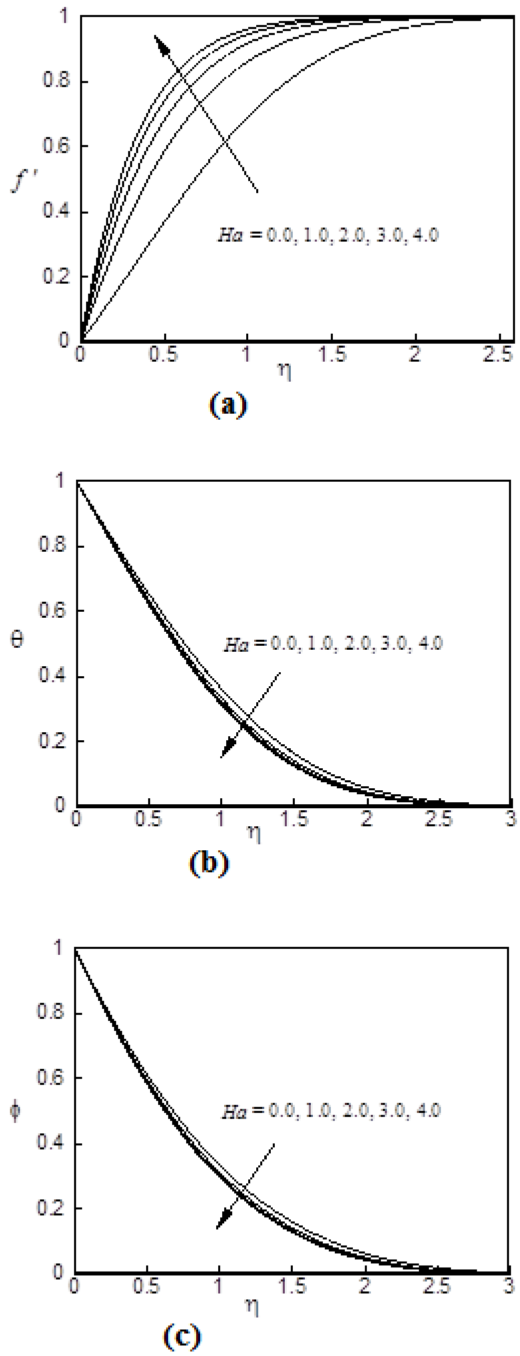

Fig. 3. Variation of dimensionless (a) velocity, (b) temperature and (c) concentration profiles for several values of Ha.

centration, respectively. Imposition of wall fluid suction ($f_w > 0$) for this problem has the effect of reducing the entire hydrodynamic, thermal and concentration boundary layers causing the fluid velocity to increase while decreasing its temperature and concentration. On the other hand, imposition of wall fluid injection ($f_w < 0$) produces the opposite effect. The decreasing thickness of the concentration layer is caused by two effects (i) the direct action of suction, and (ii) the indirect action of suction causing a thinner thermal boundary layer, which corresponds to the higher temperature gradient, a consequent increase in the thermophoretic force and higher concentration gradient.

Fig. 3 (a)-(c) respectively show the typical velocity, temperature and concentration profiles against η for various values of the Hartman number Ha. Fig. 3 (a) presents significant impact of the applied magnetic field on the flow field. The x-direction velocity increases hence thickness of the hydrodynamic boundary layer decreases with the increase of the Hartman number Ha. This is due to the fact that the application of a magnetic field moving with the free stream has the tendency to induce a electromotive force, which increases the motion of the fluid. On the other hand the temperature and concentration of the fluid within the boundary layer decrease with the increase of Hartman number Ha. It can further be noted that the thicknessess of the thermal and concentration boundary layers decrease with the

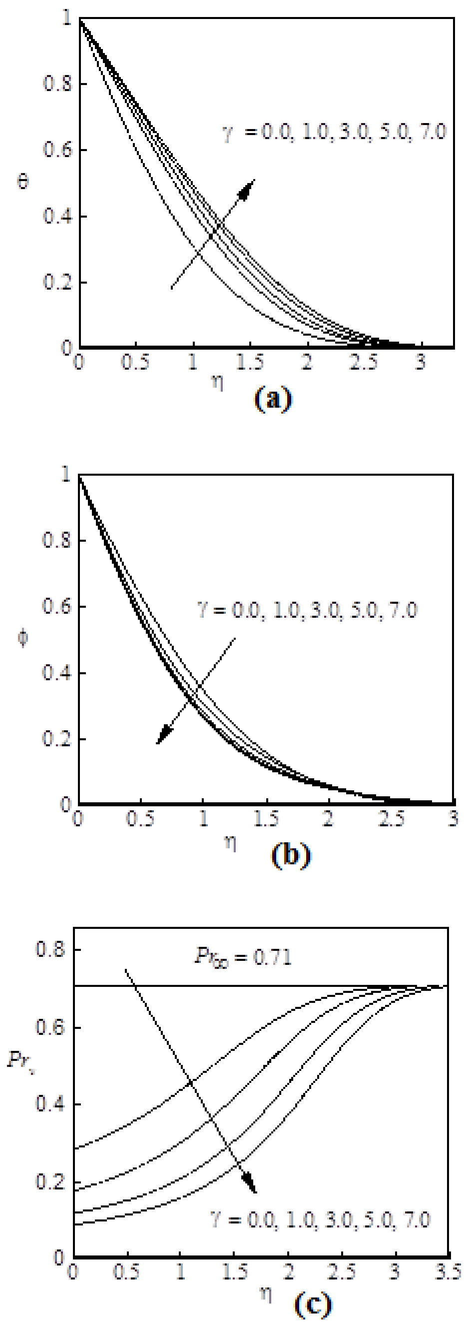

Fig. 4. Variation of dimensionless (a) temperature (b) concentration and (c) Pr_υ for several values of γ.

increase of the strength of the applied magnetic field that is consistent with the work of Ishak et al. [43].

The effects of the thermal conductivity variation parameter γ on the non-dimensional temperature profiles have been displayed in Fig. 4 (a). From this figure, we observe that the non-dimensional temperature profile increases with the increase of the thermal conductivity parameter as expected. The value $\gamma = 0$ corresponds to the constant conductivity of the fluid. Thus for the constant conductivity of the fluid the surface temperature is found to be lower compared to the variable conductivity. This can be explained as; when γ increases i. e. thermal conductivity of the fluid increases, the value of the Prandtl number decreases (see Eq. (27)) which then increases the temperature of the fluid. That is temperature of the fluid increases, if the Prandtl number decreases. On the other hand, from Fig. 4 (b), we see that the dimensionless concentration profiles decrease with the increase of the thermal conductivity parameter. From Fig. 4 (c), it is also found that Pr_υ decreases with the increase of the thermal conductivity parameter γ. This figure clearly establishes that the Prandtl number varies significantly within the boundary layer when the fluid thermal conductivity varies with temperature.

The effect of the unsteadiness parameter λ on the dimensionless velocity within the boundary layer is shown in Fig. 5 (a). From this figure we observe that for large values of λ that is for higher unsteadiness, separation occurs even

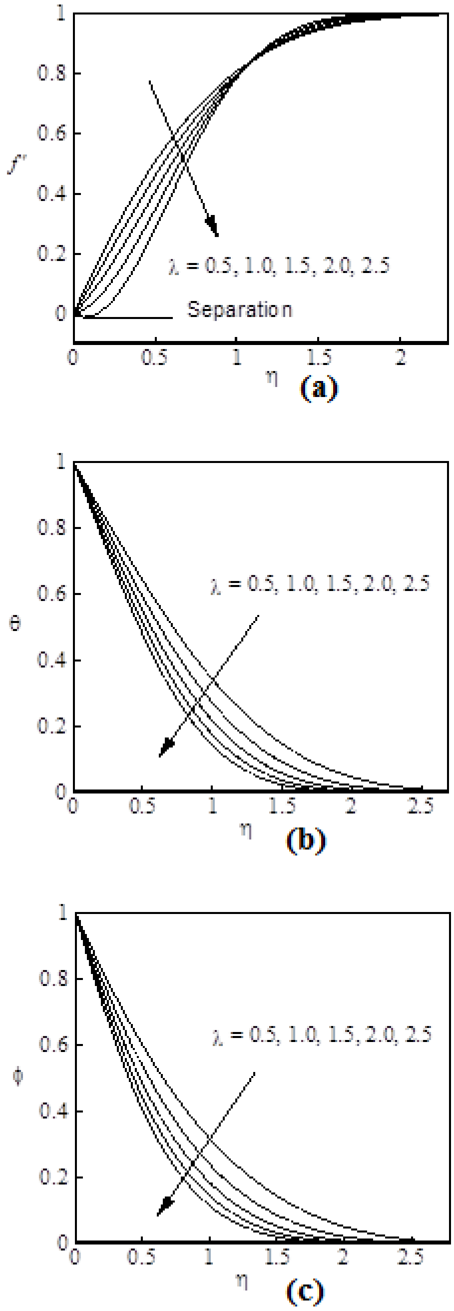

Fig. 5. Variation of dimensionless (a) velocity, (b) temperature and (c) concentration profiles for several values of unsteadiness parameter λ.

in the case of accelerated flow or of adverse pressure gradient ($\beta > 0$). Velocity here is also found to be decreased with the increase of λ within some domain $\eta \leq \eta_{critical}$ and then for $\eta > \eta_{critical}$ the tendency is reversed in the upper portion of the boundary layer. Similar behavior has been also observed by Sattar [29]. Fig. 5(b)-(c), respectively, depict the non-dimensional temperature and concentration, respectively within the boundary layer for different values of the unsteadiness parameter λ. From these figures, we observe that both temperature and concentration decreases with the increasing values of the unsteadiness parameter λ.

The variation of dimensionless concentration inside the boundary layer for various values of the Schmidt number Sc , thermophoresis parameter N_t and thermophoretic coefficient κ are displayed in Fig. 6 (a)-(c), respectively. From these figures, we observe that concentration profiles within the boundary layer increases with the increasing values of the thermophoretic coefficient whereas it decreases with the increasing values of both Sc and N_t.

The combined effects of Ha and N_t, γ and N_t, κ, and N_t on thermophoretic velocity ($V_{TW} Re^{-\frac{1}{2}}$) are shown in Fig. 7(a)-(c), respectively. From these figures, we see that the thermophoretic velocity is increased with the increasing values of Ha and κ while it decreases with the increasing values of the thermal conductivity parameter γ and the ther-

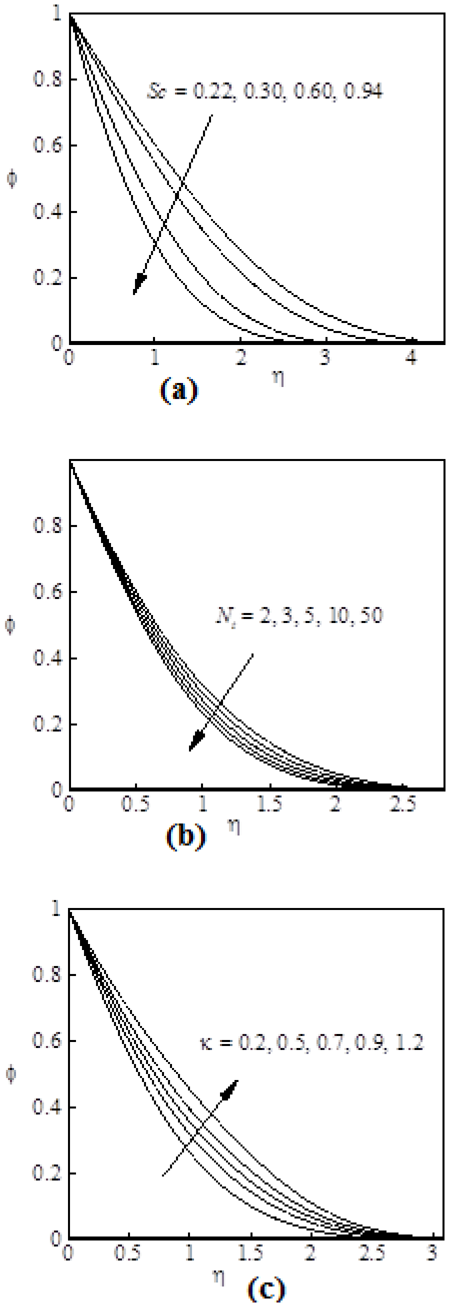

Fig. 6. Variation of dimensionless concentration profiles for various values of (a) Sc (b)N_t and (c)κ .

mophoresis parameter N_t. For the variable Prandtl number Pr_v the values of $(V_{TW}Re^{-\frac{1}{2}})$ are higher corresponding to the values when the Prandtl number is kept constant.

Table 3 shows the variations of the thermophoretic particle deposition velocity $(V_d^* Re^{-\frac{1}{2}})$ at the wedge surface for various values of Schmidt number for both suction $(f_w > 0)$ as well as injection $(f_w < 0)$ cases. From this table, we observe that the thermophoretic particle deposition velocity decreases with the increase of the Schmidt number for both suction as well as injection. For experimental interest, the thermophoretic particle deposition velocity decreased by 50.95% and 64.93% when the Schmidt number increased from 0.22 to 0.94 for both suction as well as injection.

The significance of the thermal conductivity parameter on the rate of heat transfer for both variable Prandtl number (VPr) and constant Prandtl number (CPr) is displayed in Table 4 for both suction $(f_w > 0)$ as well as injection $(f_w < 0)$ cases. From this table, it is found that in both cases, the rate of heat transfer $(-\theta'(0))$ for the variable Prandtl number (VPr) case is higher than the constant Prandtl number (CPr) case, and the absolute error between them increases significantly with the increase of γ .

Therefore, consideration of Prandtl number as constant within the boundary layer for variable thermal conductivity is unrealistic. It is also found that the heat transfer rate decreased by 45.18% when the thermal conductivity

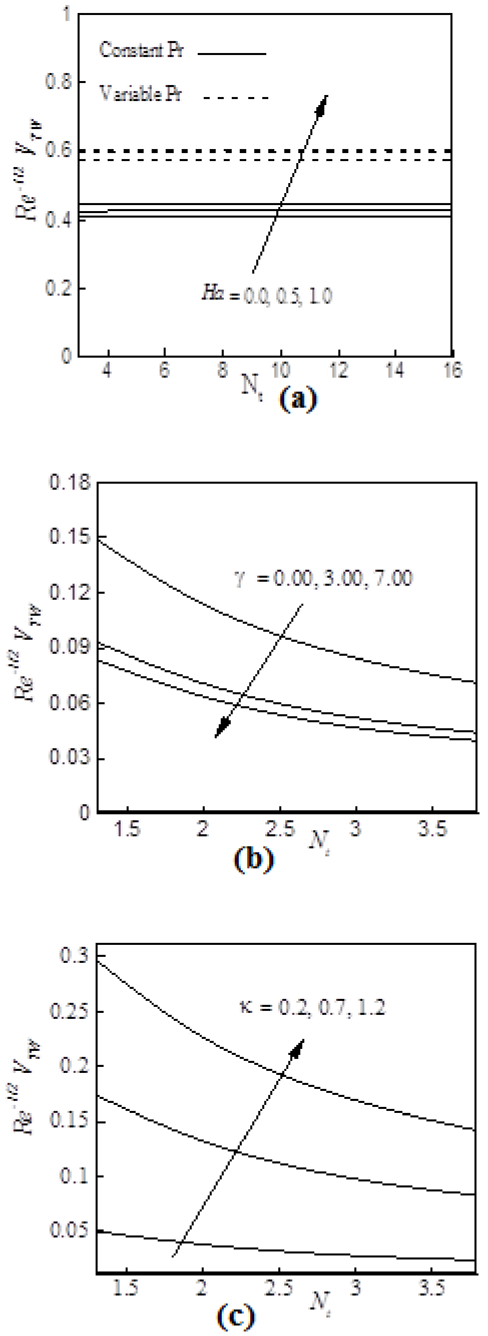

Fig. 7. Variation of thermophoretic velocity for various values of (a) Ha and N_t , (b) γ and N_t , and (c) κ and N_t .

variation parameter (γ) varies from 0 to 9 for variable Prandtl number case, whereas the corresponding decrease is 76.56% when the Prandtl number is treated as constant.

9. Conclusions

In this study effect of magnetic field and thermophoresis particle deposition on unsteady forced convective heat and mass transfer flow along a porous wedge taking into account the temperature dependent thermal conductivity and variable Prandtl number has been analyzed numerically. A comparison with previously published work was performed, and the results were found to be in excellent agreement. From the present numerical computations, the following major conclusions may be listed:

- Magnetic field moving with the free stream has the tendency to induce an electromotive force which increases the motion of the fluid and decreases its boundary layer.
- Suction or injection strongly controls the growth of the boundary layer.
- Thermophoretic velocity ($V_{TW} Re^{-\frac{1}{2}}$) is increased with the increasing values of the magnetic field parameter Ha , and thermophoretic coefficient κ while it decreases with the increasing values of the thermal conductivity variation parameter γ , and the thermophoresis parameter N_t.
- Thermophoretic particle deposition velocity ($V_d^* Re^{-\frac{1}{2}}$) increases by the increase of Schmidt number Sc. It is also mentioned that thermophoretic particle deposition velocity decreased by 50.95% and 64.93% when the Schmidt number increased from 0.22 to 0.94.
- Heat transfer rate decreased by 45.18% when the thermal conductivity variation parameter varies from 0 to 9 when Prandtl number is variable, whereas the corresponding decrease is 76.56% when the Prandtl number is treated as constant within the boundary layer.
- In any physical model where thermal conductivity of the fluid is temperature dependent, the Prandtl number within the boundary layer must be treated as variable rather than constant.

Nanofluids are a new class of fluids which can be used for various purposes specially for solar collectors to improve the efficiency of the collector. The interdisciplinary nature of nanofluids research presents a great opportunity for exploration and discovery at the frontiers of nanotechnology. An investigation is under way exploring the heat transfer augmentation considering nanofluids in the present model.

References

[1] P. Goldsmith, F.G. May, Diffusiophoresis and thermophoresis in water vapor system, in: C.N. Davies (Ed.), Aerosol Science, Academic Press, London, 1966.
[2] T. Kanki, S. Luchi, T. Miyazaki, H. Udea, On thermophoresis of relatively large aerosol particles suspended near a plate, J. Colloid., Interf. Sci. 107 (1985) 418-425.
[3] C. Shen, Thermophoretic deposition of particles onto cold surface of bodies in two-dimensional and axi-symmetric flows, J. Colloid., Interf. Sci. 127 (1988) 104-115.
[4] K. Vajravelu, J. Nayfeh, Hydromagnetic convection at a cone and a wedge, Int. Communications in Heat and Mass Transfer 19 (1992) 701-710.
[5] A.G. Konstandopoulos, Effect of particle inertia on aerosol transport and deposit growth dynamics, PhD dissertation, Chemical Engineering, Yale University, New Haven, Connecticut, USA, 1991.
[6] Y.P. Chang, R. Tsai, F.M. Sui, The effect of thermophoresis on particle deposition from a mixed convection flow onto a vertical flat plate, J. Aerosol Sci. 30 (1999) 1363-1378.
[7] S.P. Anjjali Devi, R. Kandasamy, Thermal stratification on laminar boundary layer flow over a wedge with suction or injection, Mech. Res. Commun. 28 (3) (2001) 349-354.
[8] A.J. Chamkha, I. Pop, Effects of thermophoresis particle deposition in free convection boundary layer from a vertical flat plate embedded in a porous medium, Int. Communications in Heat and Mass Transfer 31 (2004) 421-430.
[9] A.J. Chamkha, Al- Mudhaf, F. Ali, Effect of heat generation or absorption on thermophoretic free convection boundary layer from a vertical flat plate embedded in a porous medium, Int. Communications in Heat and Mass Transfer 33 (2006) 1096-1102.
[10] A. Postelnicu, Effects of thermophoresis particle deposition in free convection boundary layer from a horizontal flat plate embedded in a porous medium, Int. J. Heat and Mass Transfer 50 (2007) 2981-2985.
[11] M.S. Alam, M.M. Rahman, M.A. Sattar, Effects of variable suction and thermophoresis on steady MHD combined free-forced convective heat and mass transfer flow over a semi-infinite permeable inclined flat plate in the presence of thermal radiation, Int. J. Thermal Sci. 47 (2008) 758-765.
[12] M.M. Rahman, A. Postelnicu, Effects of thermophoresis on the forced convective laminar flow of a viscous incompressible fluid over a rotating disk, Mech. Res. Commun. 37 (2010) 598-603.

[13] G. Konstandopoulos, D.E. Rosner, Inertia effects on thermophoretic transport of small particles to walls with stream wise curvature, Part-I: Theory, Int. J. Heat and Mass Transfer 38 (1995) 2305-2315.

[14] R. Tsai, A simple approach for evaluating the effect of wall suction and thermophoresis on aerosol particle deposition from a laminar flow over a flat plate, Int. Communications in Heat and Mass Transfer 26 (1999) 249-257.

[15] M.S. Alam, M.M. Rahman, On the effectiveness of variable heat and mass fluxes on hydromagnetic free convection and mass transfer flow along an inclined permeable stretching surface with thermophoresis, Int. j. Energy and Technology 5 (1) (2013) 1-10.

[16] T. Watanabe, I. Pop, Magnetohydrodynamic free convection flow over a wedge in the presence of a transverse magnetic field. Int. Communications in Heat and Mass Transfer 20 (1993) 871-881.

[17] P. Chandran, N.C. Sacheti, A.K. Singh, Hydromegnetic flow and heat transfer past a continuously moving porous boundary. Int. Communications in Heat and Mass Transfer 23 (1996) 889-898.

[18] K. A. Yih, MHD forced convection flow adjacent to a non-isothermal wedge. Int. Communications in Heat and Mass Transfer 26 (1999) 819-827.

[19] K.A. Yih, Free convection effect on MHD coupled heat and mass transfer of a moving permeable vertical surface. Int. Communications in Heat and Mass Transfer 26 (1999) 95-104.

[20] ATM. M. Rahman , M.S. Alam , M.A. Alim, M.K. Chowdhury, Unsteady MHD forced convective heat and mass transfer flow along a wedge with variable electric conductivity and thermophoresis, Procedia Engineering, 56 (2013) 531-537.

[21] I. Muhaimin, R. Kandasamy, A. B. Khamis, R. Rozaini, Influence of thermophoresis particle deposition and chemical reaction on unsteady non-Darcy MHD mixed convective flow over a porous wedge in the presence of temperature dependent viscosity, J. Mechanical Science and Technology 27 (5) (2013) 1545-1555.

[22] T.C. Chiam, Heat transfer with variable conductivity in a stagnation-point flow towards a stretching sheet, Int. Communications in Heat and Mass Transfer 23 (1996) 239-248.

[23] T.C. Chiam, Heat transfer in a fluid with variable thermal conductivity over a linearly stretching sheet, Acta Mech. 129 (1998) 63-72.

[24] K.V. Prasad, K. Vajravelu, Heat transfer in the MHD flow of a power law fluid over a non-isothermal stretching sheet, Int. J. Heat and Mass Transfer 152 (2009) 4956-4965.

[25] M.S. Abel, Siddheshwar, N. Mahesha, Effects of thermal buoyancy and variable thermal conductivity on the MHD flow and heat transfer in a power-law fluid past a vertical stretching sheet in the presence of a on-uniform heat source, Int. J. Non-Linear Mech. 44 (2009) 1-12.

[26] K. Vajravelu, K.V. Prasad, Chiu-On Ng, Unsteady convective boundary layer flow of a viscous fluid at a vertical surface with variable fluid properties, Nonlinear Analysis: Real World Applications 14 (2013) 455-464.

[27] M.M. Rahman, A. Aziz and M. Al-Lawatia, Heat transfer in micropolar fluid along a inclined permeable plate with variable fluid properties, Int. J. Thermal Sci. 49 (2010) 993-1002.

[28] M.M. Rahman, I.A. Eltayeb, Convective slip flow of rarefied fluids over a wedge with thermal jump and variable transport properties, Int. J. Thermal Sci. 50 (2011) 468-379.

[29] M.A. Sattar, A local similarity transformation for the unsteady two-dimensional hydrodynamic boundary layer equations of a flow past a wedge, Int. J. Appl. Math. and Mech. 7 (2011) 15-28.

[30] ATM. M. Rahman, M.S. Alam, M.K. Chowdhury, Thermophoresis particle deposition on unsteady two-dimensional forced convective heat and mass transfer flow along a wedge with variable viscosity and variable Prandtl number, Int. Communications in Heat and Mass Transfer 39 (2012) 541-550.

[31] ATM. M. Rahman, M.S. Alam, M.K. Chowdhury, effects of variable thermal conductivity and variable prandtl number on unsteady forced convective flow along a permeable wedge with suction/injection in the presence of thermophoresis, Int. J. Energy & Technology 4 (4) (2012) 1-10.

[32] L. Talbot, R.K. Cheng, A.W. Schefer, D.R. Wills, Thermophoresis of particles in a heated boundary layer, J. Fluid Mech. 101 (1980) 737-758.

[33] G.K. Batchelor, C. Shen, Thermophoretic deposition of particles in gas flowing over cold surface, J. Colloid Interface Sci. 107 (1985) 21-37.

[34] M.A. Sattar, M M. Hossain, Unsteady hydromagnetic free convection flow with Hall current and mass transfer along an accelerated porous plate with time dependent temperature and concentration, Can. J. Physics 70 (1992) 369-374.

[35] G.G. Stokes, On the effect of internal friction of fluids on the motion of pendulums, Trans Cambr. Phil. Soc. 9 (2) (1856) 8-106.

[36] H. Schlichting, K. Gersten, Boundary layer theory, Springer-Verlag, 8th Edition, 2000.

[37] M. S. Alam and M. N. Huda, A new approach for local similarity solutions of an unsteady hydromagnetic free convective heat transfer flow along a permeable flat surface, International Journal of Advanced in Applied Mathematics and Mechanics 1(2) (2013) 39-52.

[38] M. S. Alam, Transient thermophoretic particle deposition on MHD free convective and viscous dissipation flow along an inclined surface considering Dufour-Soret effects, International Journal of Advanced in Applied Mathematics and Mechanics 1(3) (2014) 121-134.

[39] M. S. Alam, M. M. Haque and M. J. Uddin, Convective flow of nanofluid along a permeable stretching/shrinking wedge with second order slip using Buongiorno's mathematical model, International Journal of Advanced in Ap-

plied Mathematics and Mechanics 3(3) (2016) 79-91.
[40] P.R. Nachtsheim, P. Swigert, Satisfaction of the asymptotic boundary conditions in numerical solution of the system of non-linear equations of boundary layer type, NASA TND-3004, 1965.
[41] M.S. Alam, M.M. Rahman, M.A. Samad , Numerical study of the combined free-forced convection and mass transfer flow past a vertical porous plate in a porous medium with heat generation and thermal diffusion, Nonlinear Analysis: Modelling and Control 11 (2006) 331-343.
[42] F.M. White, Viscous Fluid Flows, third ed. McGraw-Hill, New York, 2006.
[43] A. Ishak, R. Nazar, I. Pop, MHD boundary layer flow of a micropolar fluid past a wedge with variable wall temperature, Acta Mechanica 196 (2008) 75-86.